Survival of the thickest? – Impacts of extreme wave-forcing on marsh seedlings are mediated by species morphology

Running head: Marsh seedling response to storm waves

K. Schoutens*[1], S. Reents[2], S. Nolte[3,4], B. Evans[5], M. Paul[6,7], M. Kudella[8], T.J. Bouma[9,10], I. Möller[11], S. Temmerman[1]

[1]University of Antwerp, Ecosystem Management Research Group;

[2]University of Hamburg, Applied Plant Ecology;

[3]University of East Anglia, School of Environmental Sciences;

[4]Centre for Environment, Fisheries and Aquaculture Science;

[5]University of Cambridge, Biogeography and Biogeomorphology Group;

[6]University of Braunschweig, Department of Landscape Ecology and Environmental Systems Analysis;

[7]Leibniz University Hannover, Ludwig-Franzius-Institute for Hydraulic, Estuarine and Coastal Engineering;

[8]Forschungszentrum Küste (FZK);

[9]Netherland Institute for Sea Research (NIOZ), Yerseke Spatial Ecology;

[10]Utrecht University, Faculty of Geosciences;

[11]Trinity College Dublin, Department of Geography

*e-mail: ken.schoutens@uantwerpen.be

Abstract

Although tidal marshes are known for their coastal defense function during storm surges, the impact of extreme wave forcing on tidal marsh development is poorly understood. Seedling survival in the first season after germination, which may involve exposure to extreme wave events, is crucial for the natural establishment and human restoration of marshes. We hypothesize that species-specific plant traits plays a significant role in seedlings survival and response to wave induced stress, i.e. through stem bending and uprooting. To test this hypothesis, seedlings of pioneer species (*Bolboschoenus maritimus*, *Schoenoplectus tabernaemontani*, *Spartina anglica* and *Puccinellia maritima*) with contrasting biophysical traits were placed in the Large Wave Flume in Hannover (Germany) and exposed to storm wave conditions.

Seedlings of *P. maritima* and *S. anglica* experienced a lower loss rate and bending angle after wave exposure compared to *S. tabernaemontani* and especially *B. maritimus*. The higher loss rates of *B. maritimus* and *S. tabernaemontani* result from deeper scouring around the stem base. Scouring depth was larger around stems of greater diameter and higher resistance to bending. Here, *B. maritimus* and *S. tabernaemontani* have both thicker and stiffer stems than *S. anglica* and *P. maritima*. Our results show that especially seedlings with thicker stems suffer from erosion and scouring, and have the highest risk of being lost during extreme wave events. This implies that for successful seedling establishment and eventually the establishment of a mature tidal marsh vegetation, the species composition and their capacity to cope with storm wave disturbances is crucial.

Keywords: Seedlings, tidal marsh, storm waves, marsh establishment, scouring, drag force, plant traits, restoration, wave flume

Introduction

Understanding the mechanisms that facilitate or hinder plant establishment on tidal flats is fundamental for succesfull tidal marsh restoration and creation, which is increasingly implemented for delivery of a multitude of ecosystem services, including the nature-based mitigation of coastal hazards related to global change (Narayan et al. 2016; van der Nat et al. 2016; Oppenheimer et al. 2019). Despite being the focus of this increased attention, tidal marsh ecosystems are still under threat due to environmental change and anthropogenic pressures, such as sea level rise, and local factors, such as marsh conversion to human land use (Lotze et al. 2006; Nicholls and Cazenave 2010; Van Asselen et al. 2013).

To counteract loss or create new tidal marshes as nature based solutions, a variety of methods are used to (re-)establish ecological functioning. In practice, tidal marsh (re-)establishment requires the presence of a suitable habitat for marsh development, such as suitable bed elevation (i.e. tidal inundation frequency) and hydrodynamic conditions that allow seedling establishment and growth (Wolters et al. 2008; Zhao et al. 2020). There are several options to initiate the growth of marsh vegetation, i.e. (i) by adult propagule settlement, (ii) lateral clonal expansion of existing marsh plants or (iii) seedling establishment (Balke et al. 2014; Hu et al. 2015). Aside from a detailed understanding of the conditions under which seeds of tidal marsh plants can germinate and establish (Hu et al. 2015), it might be even more important to know how seedlings can survive energetic environments to facilitate and ensure successful marsh restoration and creation.

Studies on seedling survival often focus on the initial establishment phase, i.e. the phase where the seedlings become independent of the resources in the seed (Balke et al. 2014; Zhu et al. 2014). After initial seedling establishment in calm growing conditions, potential storm events

in the course of the growing season might exert strong mechanical stress on the developing seedlings (Paul et al. 2016; Rupprecht et al. 2017) and may limit their survival. Yet many studies on seedling survival are conducted under relatively low levels of hydrodynamic exposure (Silinski et al. 2015; Cao et al. 2018, 2020; Xie et al. 2019). In contrast, little is known about survival in the period between initial seedling establishment and fully grown, patch forming pioneer vegetation, when the plants could still be vulnerable to more extreme hydrodynamic disturbances. On the one hand storm surges are difficult to investigate in the field due to their sporadic nature and relative unpredictability in terms of timing of occurrence, magnitude and precise meteorological characteristics (Hansen et al. 2019). On the other hand storm surges and storm waves are difficult to simulate in lab conditions without encountering significant scaling issues (Spencer et al. 2015; Masselink et al. 2016).

Fundamental knowledge on the processes that determine seedling survival under storm conditions is required to support the implementation of successful restoration of tidal marshes and their valuable ecosystem services. Structural failure of plants due to hydrodynamic stress is initiated by (1) drag forces acting on the plant shoots (Henry et al. 2015; Paul et al. 2016) and can be facilitated by (2) sediment scour around the stem base (Friess et al. 2012). Drag forces result from friction between the water flow and the plant shoot (e.g. Dalrymple and Dean 1991; Denny 1994), which is known to be a function of hydrodynamic forces (i.e. flow velocities), plant morphology (i.e. shoot surface area) and stem biomechanical properties (i.e. stem stiffness) (Paul et al. 2016; Vuik et al. 2018). Recent studies highlight that such species-specific plant traits also affect the plant's capacity to cope with mechanical stress from hydrodynamic forces (Silinski et al. 2018; Schoutens et al. 2020). For example, if the drag forces exceed the shoots' resistance against breakage, the stem will buckle or will break which can be fatal for the survival of the plant (Vuik et al. 2018). Moreover, when drag forces exceed the root anchoring strength, the seedling will be dislodged and will be flushed away by waves

and currents. For the anchoring strength of the seedling, the root growth and structure are crucial (Peralta et al. 2006; Szmeja and Galka 2008). Additionally, anchoring strength decreases through the development of scour holes around the stem base resulting from turbulence, leading to reduced contact area between roots and soil. Scour hole volume around single shoots has been shown to be a function of hydrodynamic forces, morphological and biomechanical plant properties (Bouma et al. 2009a), and sediment properties (Lo et al. 2017). Additionally, scouring around patches of multiple shoots growing close to each other, has been reported to depend also on the shoot density within the patch (e.g. Bouma et al. 2009b; Duggan-Edwards et al. 2020). When scour decreases the anchoring strength up to a point where drag forces can dislodge the complete plant, it will be flushed away and lost (Clark et al. 2015). The role of plant traits on drag forces and scouring processes during storm wave conditions remains unclear.

In the present study we experimentally assess the survival rates of four different species of pioneer tidal marsh seedlings with distinct morphologies, under storm wave conditions. More specifically, we examine the cause of structural failure, i.e. stem bending and uprooting by storm waves and how this relates to species-specific plant traits. Drag force proxies and scouring were quantified. Plant morphological and biomechanical properties were measured to support discussion of potential explanations of species differences in survival, damage, scouring and drag forces. With this discussion we aim to increase insights into the link between species-specific plant traits and the capacity of the seedlings to survive storm wave conditions.

Methods

Studied species

To test the hypothesis that plant traits exert a significant influence on the survival of pioneer marsh seedlings under storm wave conditions, four NW European pioneer marsh species with distinct morphologies were selected: *Bolboschoenus maritimus* (L.) Palla, *Schoenoplectus tabernaemontani* (C.C.Gmel.) Palla, *Spartina anglica* C.E. Hubb. and *Puccinellia maritima* (Huds.) Parl. *B. maritimus* and *S. tabernaemontani* are pioneer species in brackish marshes, while *P. maritima* and *S. anglica* are found in pioneer salt marshes. All four species can spread by clonal outgrowth (via rhizomes or stolons) of existing adult plants but can also colonize bare mudflats by seed dispersal. After flowering in summer, seeds can spread by the wind or tide in autumn followed by germination in spring. *B. maritimus* is often found as pioneer species in brackish marshes forming monospecific patches/zones parallel to the marsh shoreline. They form tall, thick shoots (up to 2.5 m high) with leaves. *S. tabernaemontani* can be found in the same brackish environment of pioneer marshes (Heuner et al. 2018; Elsen et al. 2019). It grows in monospecific stands and produces tall and thick stems (up to 2.0 m high) without leaves. *P. maritimus* is typically found in pioneer (to mid-successional) salt marshes characterised by sheltered conditions. It forms dense tufts (up to 0.7 m high) of thin flexible stems with leaves spread over the soil surface. The salt marsh coloniser *S. anglica* is a pioneer that grows in dense tussocks of thin stems with leaves (up to 1.5 m high) under highly dynamic conditions often covering the lowest parts of the marsh.

Experimental setup

a. Preparation of experimental plant units

Upon stratification (4 °C during the night and room temperature during the day), germination of seeds was initiated on moist substrate. Three weeks after the start of the stratification (mid-

June 2018), the seedlings were first planted in fertilised (slow release Osmocote, Substral) sand from the Scheldt estuary (SW Netherlands) and grown in greenhouse conditions. Five weeks later, the seedlings were transplanted in large sediment boxes (120cm by 80cm, 40 cm soil depth) that were later placed in the flume. The sediment in the boxes was composed of 32% silt and clay (< 63 μm), and 31%, 11%, 24%, and 2% very fine (63 – 125 μm), fine (125 – 200 μm), medium (200 – 630 μm), and coarse sand (> 630 μm), respectively, with a mean grainsize of 152.02 μm. As the sediment comes from the intertidal zone of the Scheldt estuary, this particle size distribution is representative for tidal marshes and mudflats in this estuary. Seedlings were planted 15 cm apart in a grid of 4 by 6 with a distance of 20 cm from the front and the back and 15 cm from the sides of the sediment box to minimize interference between the individuals and still enabling plantation of a reasonable amount of individuals (24 per sediment box) in the available space of the sediment boxes to allow statistical analyses (Fig. 1). Throughout the entire preparation period, the boxes were stored outside and the substrate was kept moist by irrigation with freshwater. The seedlings were 10 to 14 weeks old during the experiment.

b. Spatial and temporal setup

The experiment was carried out over a three week period (13-31 August 2018) in the Large Wave Flume (Grosser Wellenkanal, GWK) of the Forschungszentrum Küste (FZK), Hannover, Germany. In the middle of the wave flume (310 m long, 5 m wide and 7 m deep), an elevated platform (40 m long) was split over its length into separate zones (Fig. 1). The zones (horizontally separated by 10 m of platform) consisted of lowered gaps in the platform in which sediment boxes with plants were placed so that the surface of the sediment boxes was level with the platform surface. In addition to the experiment with seedlings described in this paper, which was performed in one such zone, other sediment boxes in other zones contained parallel experiments of which the results will be reported elsewhere. In the seedling zone, four sediment

boxes were placed, each box contained 24 individual seedlings of one of the four different plant species. This set-up with sediment boxes excludes flume wall-edge erosion effects (Möller et al. 2014). One set of four boxes was placed in the flume for a whole week and then replaced by a new set of four boxes in the next week. Hence, for the three week period of the experiment, three sets of four sediment boxes filled with seedlings were prepared.

We highlight that the three consecutive weeks do not represent three replicate runs with the same wave conditions. Instead, over the three-week course of the experiment, a sequence of different wave conditions was applied (further called wave runs). Every week, four different wave runs were applied on day 2, 3, 4 and 5, with a daily increase in the intensity of simulated wave conditions (Table 1). This set-up gave us a total of 12 different wave runs covering a wide range of (extreme) hydrodynamic wave conditions. We chose this design to limit the risk of having a too narrow range of wave conditions for which either (i) all wave conditions would be too harsh and all seedlings would flush away after the first wave run or (ii) all wave conditions would be not harsh enough and none of the species would show any response. Instead, applying a wide range of wave conditions allowed us to identify species-dependent differences in seedling response. However, this choice and practical limitations (oa. in terms of time and resources) implied that we could not do replicate wave runs under exactly the same wave and plant conditions. Every daily wave run consisted of a JONSWAP wave spectrum of 1000 random waves (i.e. waves of different height and period as experienced typically on the shores of the North Sea) with an inundation depth of 1.5 m approximating storm surge conditions in temperate regions (Table 2). Wave and water depth conditions were selected to mimic conditions that (a) are typical of those experienced at marsh margins around the North Sea basin (e.g. Spencer et al. 2015)), (b) generate high bed shear stresses, but also (c) maintain relative uniformity of hydrodynamic forcing along the individual successive experimental zones on the raised platform. Only during the last wave run (on day 4 of week 3) were monochromatic waves used to allow higher time-averaged wave induced bed stresses to be simulated (see Table 1), which

could not be achieved through an irregular wave spectrum. In between the daily wave runs the flume was drained slowly over several hours in order to prevent erosion on the sediment surface and drag on the seedlings. Once the flume was drained, in between every daily wave run, the effects of the preceding inundation and wave conditions on the plant seedlings and sediment surface were measured, but the same boxes with sediments and plants were kept in the flume for 5 days. Hence, for four days (days 2-5), the seedlings and sediment surfaces were exposed to an accumulating load of wave energy resulting from the four consecutive wave runs.

Table 1. Incoming wave conditions measured at the start of the experimental platform. Significant wave height (H_s, m) and significant wave period (T_s, s) are shown per week and per wave run. Every wave run consisted of 1000 waves. Note that apart from the monochromatic waves during wave run 4 of week 3 (italics), all wave runs had randomly generated waves representative for North Sea conditions (JONSWAP spectrum).

		H_s (m)			**T_s (s)**		
		Week 1	**Week 2**	**Week 3**	**Week 1**	**Week 2**	**Week 3**
Wave run	**1**	0.30	0.68	0.68	2.58	3.80	4.02
	2	0.40	0.68	0.77	4.22	3.80	5.63
	3	0.58	0.78	0.78	3.56	5.66	5.63
	4	0.69	0.78	*0.71*	5.23	5.63	*6.00*

Table 2. Field studies with recordings of a maximum significant wave height (H_s, m) and inundation depths (h, m) at the marsh edge as compared to the conditions in this flume experiment.

Publication	***H_s (m)***	***h (m)***	***Study site***
This flume study	**0.78**	**1.5**	
Möller et al. 1999	0.58	1.39	North Norfolk Coast, UK
Ysebaert et al. 2011	0.64	1.86	Yangtze, CN
Yang et al. 2012	0.73	1.71	Yangtze, CN
Vuik et al. 2016	0.69	1.90	Western Scheldt, NL
Schoutens et al. 2019	1.00	3.85	Elbe, GE
Zhu et al. 2020	0.87	2.20	Wadden Sea Coast, NL

Hydrodynamic measurements

Wave-induced current velocities were recorded directly in front (0.30 m) of the seedling zone (Fig. 1). High-frequency (25 Hz) flow velocity measurements were conducted with Acoustic Doppler Velocimeters (ADVs) positioned in the middle of the flume width at 0.05 m above the bottom of the experimental platform. Wave gauge arrays mounted against the flume side wall were installed at the start of the experimental platform (Fig. 1). From these measurements, the significant wave height and period (mean of the highest third of recorded wave heights, H_s or wave periods T_s respectively) were derived (Table 1). Over the course of the four days for which individual seedling boxes were retained in the flume, the wave exposure of the seedlings and sediment surfaces progressively increased. The plant and sediment surface responses recorded on each day thus represent change induced through the previous day's wave run, but, for days 3, 4, and 5, the reported change is that which has resulted from all preceding wave

runs during that week, i.e. is relative to day 1 of the experiment. The accumulated wave load (action, *S*) for each wave run was calculated from the orbital flow velocities as the kinetic energy times the exposure time (i.e. number of wave oscillations times the representative wave period) and has the unit Joules-second (Js) (see supplementary info for the full method).

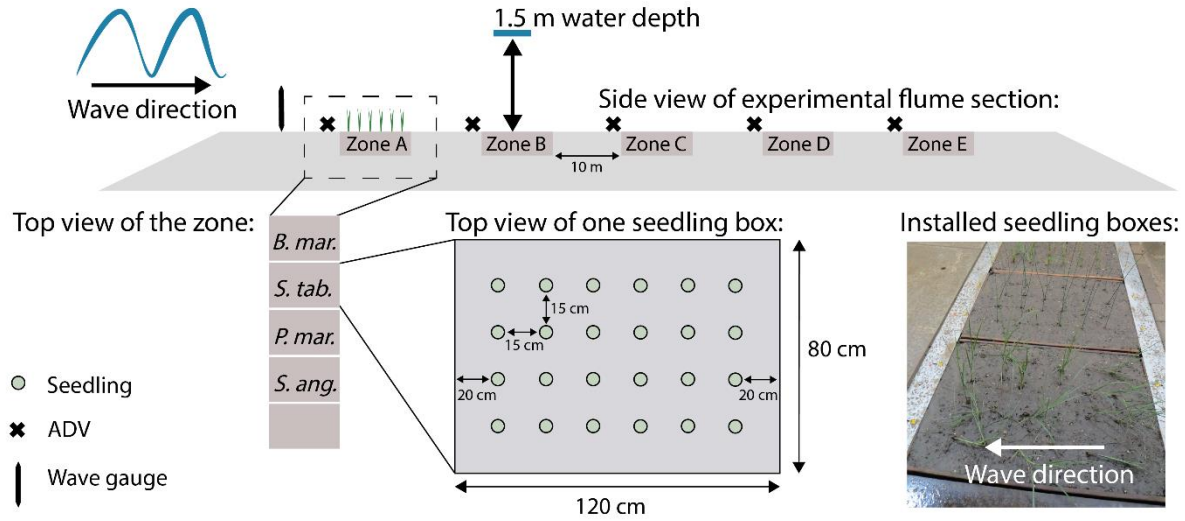

Figure 1: Schematic overview of the experimental setup in the Large Wave Flume (GWK, Hannover, Germany). On the elevated platform, installed in the flume, one zone was used to install four boxes with seedlings. Each box contained 24 seedlings of one species. The picture on the right illustrates the seedling boxes installed in the flume platform.

Plant trait dependent response to storm waves

a. Plant damage and vitality

Seedling response to storm wave exposure was quantified daily after each wave run and was compared to the initial seedling condition before the first wave run of the week. Remaining seedlings were counted and the angle, perpendicular to the sediment bed, of the standing stem was measured in categories ranging from '<18°', '18°-36°', '36°-54°', '54°-72°' and '72°-90°' (the latter representing the seedlings that were almost completely bent over on the sediment bed). Seedlings that were missing were categorised as 'lost shoot'. When a shoot was lost, the

cause (uprooting, i.e. including loss of below-ground roots; or stem breakage, i.e. below-ground roots still present) was recorded.

b. Damage resulting from drag forces and erosion

1. Scouring and erosion features

Structure from motion (SFM) photogrammetry of the sediment surfaces was used to quantify the degree of erosion, including local scouring around the individual shoots, and in certain cases larger-scale erosion features in the sediment boxes. Pictures (ca. 300) were taken daily from various angles in between wave runs, after which they were processed in Agisoft Photoscan Professional software to produce three-dimensional point clouds. For the processing of the SFM photographs to accurate ground geometry and the spatial co-registration of successive point clouds, self-adhesive fiducial markers were placed at fixed positions on metal fixings around the experimental zone. Point clouds were scaled and co-registered to a reference cloud (Day 1 of the week, before any wave run) that had previously been scaled and registered to a lower resolution (5 mm) point cloud derived from an overhead laser scanner. Comparisons between clouds were conducted using the M3C2 plugin for Cloud Compare (Lague et al. 2013). The M3C2 distances, projected onto the reference cloud, were then rasterized on a 1 mm grid prior to further analysis in R (R Core Team 2019). From this raster, the sediment elevation was extracted as rings of 2 mm thickness designated here by their outer radius. Differentiation between scour features and pallet erosion was achieved through visual inspection of images.

2. Drag forces on plants

Hydrodynamic drag forces can initiate severe mechanical stresses when applied to plant structures. It is known that such hydrodynamic drag forces depend on flow velocities, shoot biomass and shoot stiffness (Vogel 1996). In this paper, shoot biomass, shoot length and flexural stiffness were used as proxies for drag forces experienced by the four species.

Plant morphology and biomechanics

Plant morphological properties (shoot biomass, shoot length, basal stem diameter) were quantified for all four species as follows. Aboveground biomass was harvested for every surviving seedling after the last wave run of each week. Belowground biomass, as proxy for anchoring capacity, was sampled on 5 replicate seedlings per species by digging up all the roots and rinsing the sediment off. After biomass collection, the samples were dried for 72h at 70 °C and weighed. Root:shoot ratios were calculated as the mean belowground biomass divided by the mean aboveground biomass and the error bars were obtained through a propagation formula. Shoot lengths and basal stem diameters were measured on all 24 seedlings of every species each week.

Biomechanical properties (second moment of area, Young's modulus and flexural stiffness) were quantified for all four species by three-point bending tests (Niklas 1992; Rupprecht et al. 2015). Per week, 5 seedlings per species were harvested after the last wave run to test for flexural strength of the shoots. The tests were performed using a universal testing machine (Instron 5942, precision ± 0.5%) with a 10 kN load cell (Instron Corporation, Canton, MA, USA). Prior to testing, the diameters of the stems were measured with a calliper. The supports of the machine, on which the plant shoots were horizontally placed, were fixed at a distance of 15 times the stem diameter to diminish shear stress on the supports during the tests (Usherwood et al., 1997). The most basal part of the stem was placed on the two supports after which a force was applied on the centre of the stems at a displacement rate of 10 mm min^{-1}. The Instron Bluehill 3.0 software accompanied by the device creates a stress-strain curve, i.e. a graph describing the relation between vertical deflection of the stem (D; on the X-axis) and the bending force of the stem (F; on the Y-axis) which enables the calculation of the slope from the elastic deformation zone on the curve (F/D) (see supplementary info for an example of the stress-strain curve). From this slope, the flexural stiffness (EI in Nm^2) was calculated as:

(eq 1.) $EI = (s^3 F)/(48D)$,

where s is the distance between the supports. Next, the second moment of area (I in m^4), a measure for the structural geometry (i.e. shape) of the stem, was calculated. The formula used for round stems (*S. tabernaemontani, P. maritima* and *S. anglica*) is:

(eq 2.) $I = \pi r^4/64$,

where r is the diameter of the stem's cross section, and the formula for the triangular stems of *B. maritimus* is:

(eq 3.) $I = bh^3/36$,

where b is the base and h is the height of the triangular cross section. Using the flexural stiffness and the second moment of area, we calculated Young's modulus (E in N/m^2), which is a measure for the strength of the stem material, as E = EI/I.

Data analysis

Probabilities of damage were compared between species with two-proportion z-tests. Species-specific differences in scouring depth in response to storm wave conditions as well as species differences in plant traits (morphological and biomechanical properties) were tested with one-way ANOVAs or the non-parametric alternative Kruskal-Wallis test. These were followed by a multiple pairwise comparison with a post-hoc Tukey honest significant difference test or with a non-parametric pairwise comparison using Wilcoxon rank sum test with Bonferroni correction. Linear regression was applied to check for a relationship between scour depth and stem diameter and Pearson correlation coefficient was calculated. To test if shoot length is important for the risk of getting damaged we used a logistic mixed effect model with 'damage' after the 4^{th} wave run of the week as the response variable ('damaged' and 'not damaged'), the 'week' of the experiment was added as random variable and 'species' was added as random

variable nested in ‘week’. The significance of the shoot length was tested with a Likelihood Ratio test (Zuur et al. 2009). All statistical analyses were performed in R 3.5.3 (R Core Team 2019) applying a significance level of $p < 0.05$ for all tests. Normality of the residuals was tested based on visual inspection with histograms and Q-Q plots and homogeneity of variance was tested with scale-location plots. To meet normality assumptions, a log transformation was applied to the aboveground biomass data.

Results

Storm wave induced damage

Simulated storm waves had an increasing significant wave height H_s every consecutive wave run in a week (Table 1). The waves had an H_s ranging from 0.30 m up to 0.78 m and a significant wave period T_s ranging between 2.6 s and 6.0 s. As seedlings were exposed to 4 consecutive wave runs in one week, the experienced stress on any specific day was the result of the effect of any preceding wave runs that week, including the run on the day of, and preceding, the measurement of plant characteristics. Thus, the accumulated wave load was calculated (Fig. 2). With an accumulated wave load of 819 Js, the first week represented the calmest storm conditions of the experiment. The accumulated wave load in week 2 (1667 Js) and week 3 (1454 Js) were similar to each other, although the specific wave characteristics differed (Table 1).

After exposure to storm-wave conditions, the damage (i.e. stem bending angle and seedling loss) observed was highest for the *B. maritimus* and *S. tabernaemontani* seedlings (Fig. 2). Seedlings of *S. anglica* and *P. maritima* hardly showed noticeable damage, while up to 100 % of the *B. maritimus* seedlings showed damage from wave exposure. The main damage in *B. maritimus* were bent shoots and over the three weeks less than 15 % of the shoots were lost. *S.*

tabernaemontani seedlings had better survival rates and after four wave runs, the *S. tabernaemontani* seedlings had more than 57 % chance to remain upright in contrast to 26 % for *B. maritimus* seedlings (z-test Chi-squared = 13.18, df = 1, $p < 0.05$). Most damage in *S. tabernaemontani* seedlings only started from wave run 3 onwards, but was still limited, i.e. after the fourth wave run, *S. tabernaemontani* seedlings had less than 15 % chance of being bent by > 72° while this was more than 40 % for *B. maritimus* seedlings (z-test Chi-squared = 10.04, df = 1, $p < 0.05$). Interestingly, all seedlings that were lost suffered from stem breakage, mainly at the base of the stem. No cases were observed of seedlings that were uprooted, i.e. completely eroded and washed away including their roots. Apart from some exceptions, the stems bent or broke at the stem-root connection.

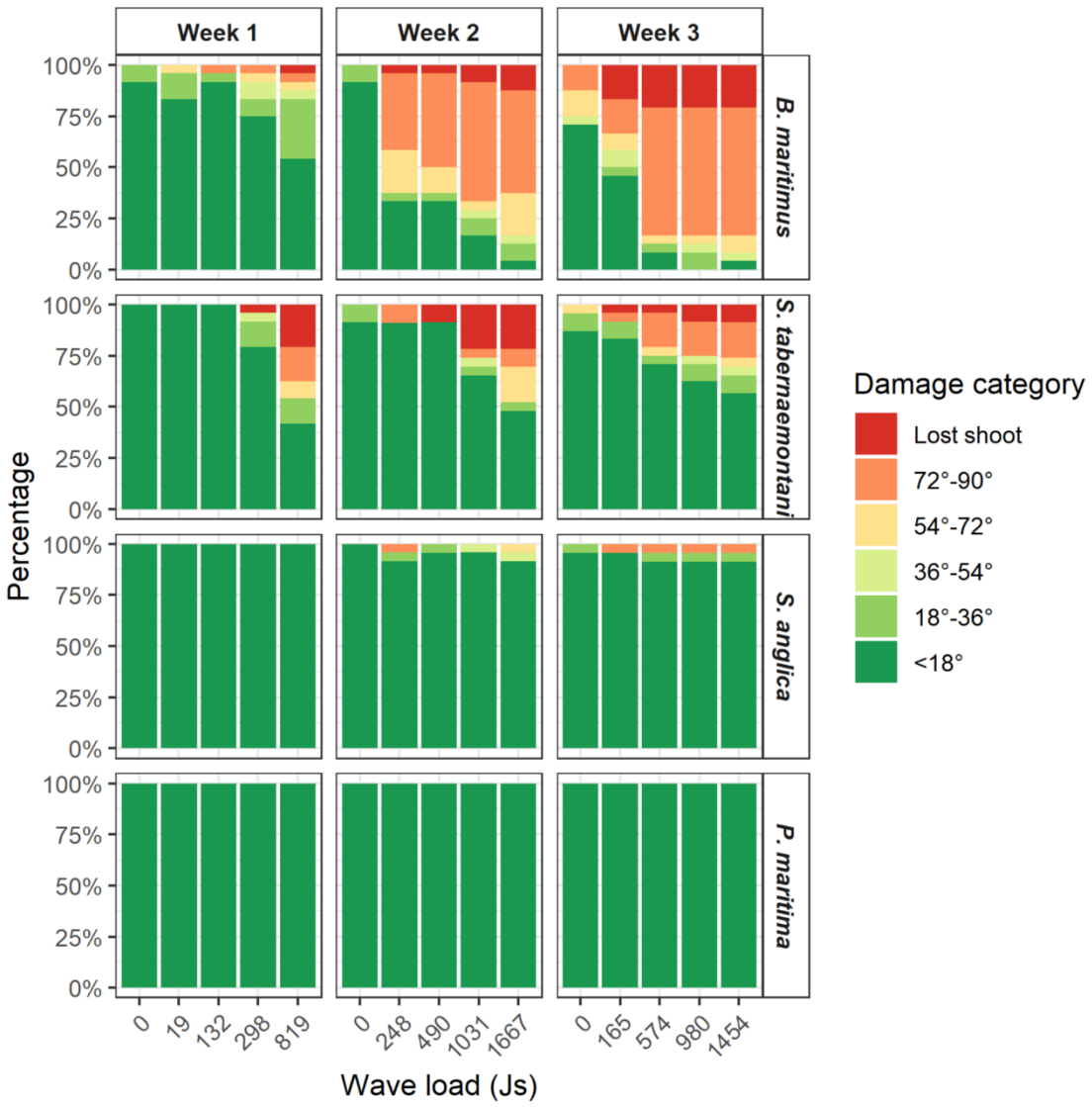

Figure 2. Percentage of seedlings (n = 24) that experienced damage caused by storm-wave exposure for the four species. Damage is quantified in six categories ranging from < 18° (i.e. no or negligible damage), to higher bending angles (increasing damage), to completely lost shoots (due to breakage at the stem base). The first day represents the initial starting situation before any wave exposure (wave load is zero). The accumulated wave load (Js) after each daily wave run is indicated on the x-axis.

Scouring processes

To gain insights in why damage differs between the species, we investigated two groups of processes that can generate wave-induced damage to the plants: (1) proxies for drag forces and (2) erosion processes such as scouring. Measurements of sediment scouring around individual plant stems, induced by turbulence, indicate a difference between species (Kruskal-Wallis Chi-squared = 128.5, df = 1, $p < 0.05$) that is in line with the observed species differences in seedling damage (Fig. 3). Especially close to the seedling stems, *B. maritimus* and *S. tabernaemontani* produced deeper scour holes (median values of 1.0 cm) compared to *P. maritima* and *S. anglica* (only a few millimeter). The scour holes around *P. maritima* were shallower and narrower compared to the scour holes around *B. maritimus* and *S. tabernaemontani*. Least scour was observed around *S. anglica*. Around some of the seedlings, the sediment was slightly elevated (in the order of magnitude of a few millimeters), which may be within registration errors, due to small deposition of elsewhere eroded sediments or due to slight swelling of the clay and silt rich sediment surface during the experiment.

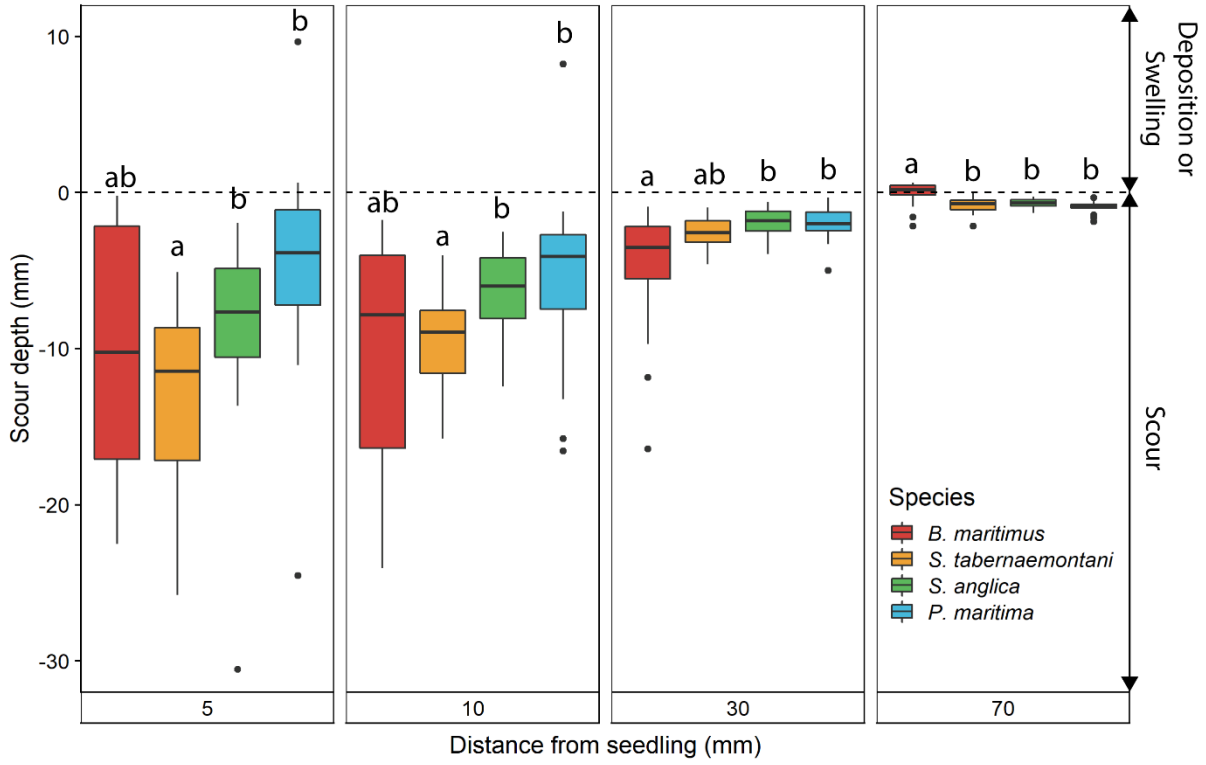

Figure 3. Median scour depth at four circular distances from the seedlings plotted as boxplots per species at the end of the 4th wave run of week 3 (i.e. the week with most extreme wave conditions) (n = 72). Erosion features, not linked to scour around the seedlings, are not shown in this figure, i.e. edge erosion induced from the edge of the sediment box or erosion induced by a pebble in the sediment. Different letters indicate significant differences as obtained by a non-parametric pairwise comparison using Wilcoxon rank sum test with Bonferroni correction.

Link between damage and erosion processes

In general, the seedlings that were not damaged did not suffer from strong erosion features, even after several wave runs (Fig. 4). *B. maritimus* seedlings that were lost due to shoot breakage at the stem base showed relatively shallow (< 10 mm) erosion features in contrast to the seedlings of *S. tabernaemontani* (> 10 mm) that were lost also due to shoot breakage. The deeper erosion features around *B. maritimus* seedlings were observed around seedlings that suffered from damage by stem bending but where the shoot was still attached. Each successive

wave run resulted in higher bending angles which were also corresponding with deeper erosion features. This pattern was less pronounced in *S. tabernaemontani*, however it should be noted that the number of seedlings suffering from damage by bending were low for this species. The *S. tabernaemontani* seedlings that did suffer damage, showed an increase in erosion depth in the last wave run of the week. In general, when a shoot started to show damage, this coincided with a step-wise change to much higher bending angles (bending angle > 18°) bypassing intermediate bending angle categories. Partial uprooting was observed for multiple seedlings, however all roots remained anchored in the sediment and hence no complete root dislodgement was recorded (see supplementary figure 1).

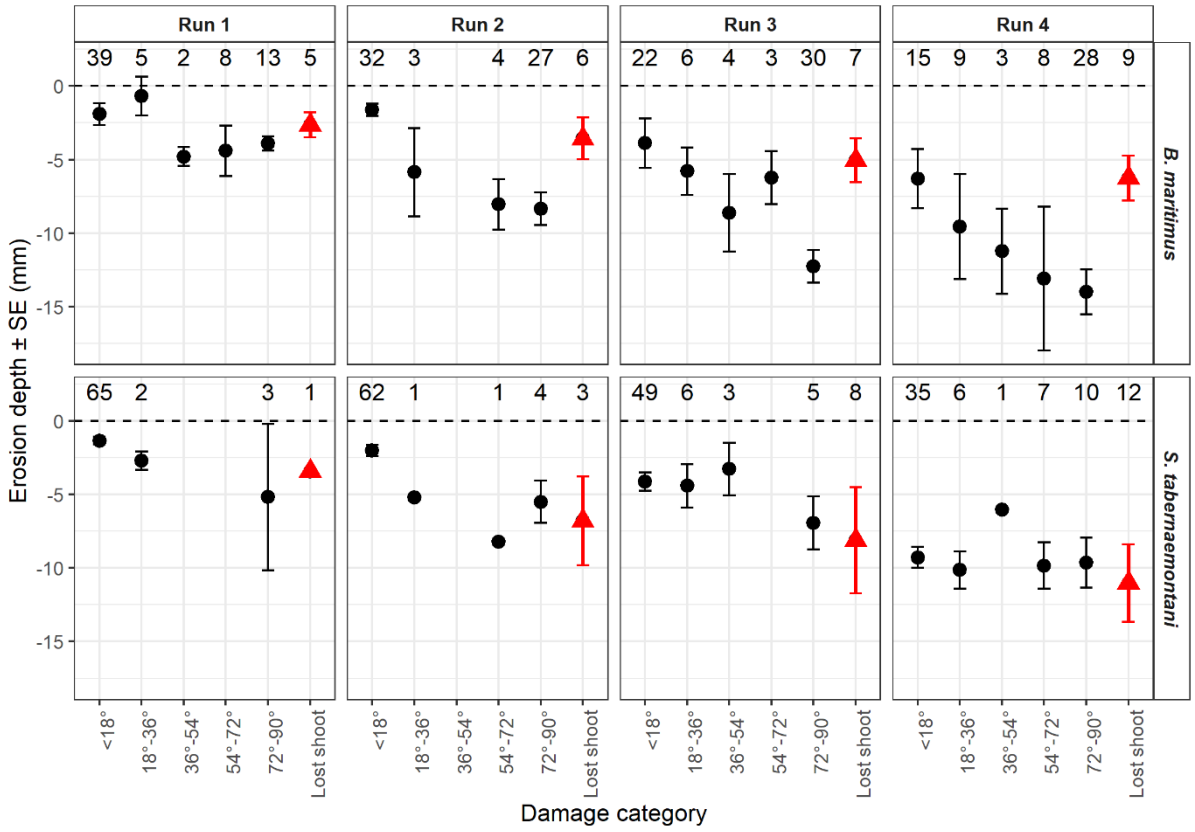

Figure 4. Mean erosion depth (mm ± SE) at 10 mm from the seedling per damage category for *B. maritimus* and *S. tabernaemontani* plotted per wave run, pooled over the three weeks to increase the number of observations in every damage category. The numbers indicate the count

of seedlings per calculated mean. Shoots that were lost by breakage at the stem base are indicated with red triangles.

In order to explore species differences in scouring depth, we further investigated species differences in plant traits that were expected to affect the scour intensity around plants, i.e. basal stem diameter and stem flexibility. Basal stem diameters of *B. maritimus* and *S. tabernaemontani* were similar to each other and significantly larger than for the other two species (Fig. 5a). *P. maritima* had the lowest stem diameter (mean of 0.9 mm), however it should be noted that seedlings of *P. maritima* sprout multiple stems and leaves from the crown. Three-point-bending tests showed that in agreement with these thicker diameters for *B. maritimus* and *S. tabernaemontani*, their second moment of area was significantly bigger than for *S. anglica* and *P. maritima* (Fig. 6c). Since no species differences in Young's modulus were found except for the higher values of *P. maritimus* during the three-point bending test, the flexural stiffness of *B. maritimus* and *S. tabernaemontani* was higher, causing higher resistance against bending with the flow (Fig. 6a-b).

Proxies for drag force and anchoring capacity

Plant traits were used as proxy for drag force to explain species differences in damage. Shoot length was highest for *S. tabernaemontani* seedlings followed by *B. maritimus* (Fig. 5b). Both species had a significantly longer shoot length (almost double the length) compared to *S. anglica* and *P. maritimus*. Seedlings that suffered from damage had significantly longer shoots compared to the seedlings that remained upstanding (damage category < 18°) (Likelihood ratio test: Chi-squared = 5.07, df = 1 $p < 0.05$). Aboveground dry biomass of *B. maritimus* seedlings collected after the 4th wave run of the week was more than twice as high (average of 0.52 ± 0.04 g per seedling) as compared to the other species (Fig. 5c). There was a non-significant difference in aboveground biomass between *S. tabernaemontani* and *S. anglica* (Tukey HSD p

= 0.1). The aboveground biomass of *P. maritima* was lowest compared to the other species. Both shoot length and aboveground biomass indicate a higher drag force for *B. maritimus* and *S. tabernaemontani* and lowest drag force for *P. maritima*. In addition to the morphological proxies for drag force, the biomechanical proxy, i.e. flexural stiffness (described above), are in line with this result (Fig. 6a). Higher resistance against breaking (i.e. higher flexural stiffness) of *B. maritimus* and *S. tabernaemontani* indicate higher drag forces compared to *S. anglica* and *P. maritima* that both have low resistance against bending (low flexural stiffness).

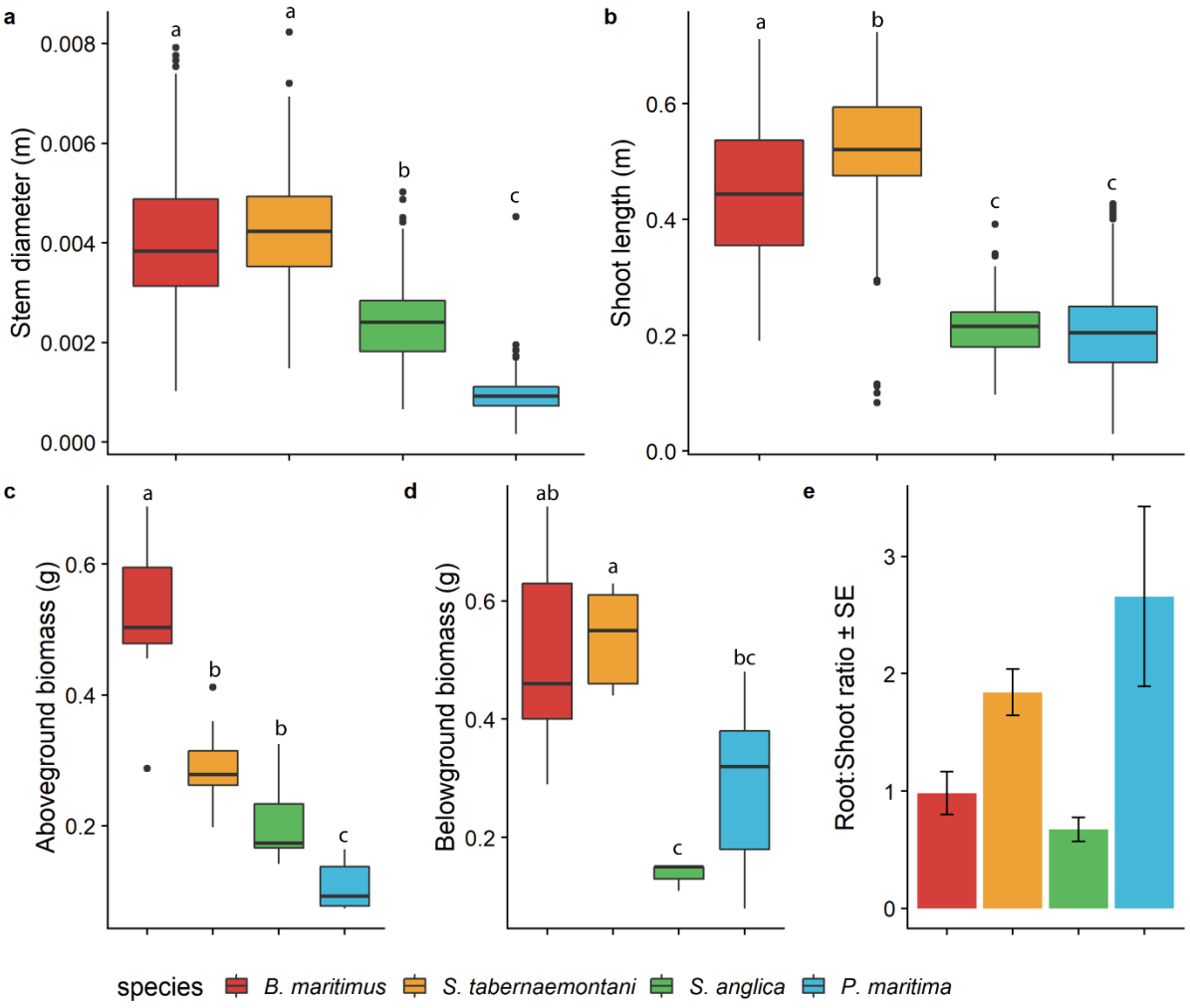

Figure 5. Plant morphogical properties as proxy for drag forces and driving force for scour. (a) Basal stem diameter and (b) shoot length per species (n = 72) are plotted as boxplots. (c) Aboveground dry biomass per seedling (n=8) and (d) belowground dry biomass per seedling

(n=5) are plotted as boxplots and (e) root:shoot ratios per species ± SE (n = 1). Letters indicate the significant differences obtained by one-way ANOVAs followed by a post-hoc Tukey HSD test.

Belowground biomass was biggest for *B. maritimus* and *S. tabermaeomontani* (Fig. 5d). Root:Shoot ratios indicate highest investment in root biomass for *S. tabernaemontani* and *P. maritima* seedlings which invested twice as much biomass in belowground parts compared to investments in shoots (Fig. 5e). In contrast to the absolute values for dry belowground biomass, *B. maritimus* invested a similar amount of biomass in its aboveground and belowground parts. *S. anglica* seedlings invested less in belowground biomass as the root:shoot ratio was below one.

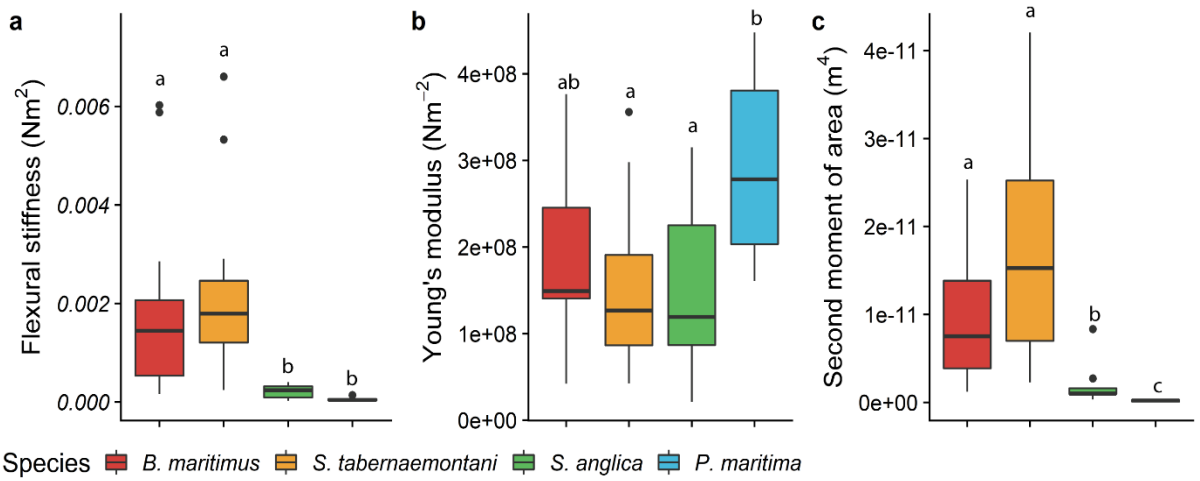

Figure 6. Biomechanical properties per species sampled over the three weeks represented as boxplots (n is, respectively, 15 for *B. maritimus* and *S. tabernaemontani* and 13 for *S. anglica* and *P. maritima*). Letters indicate the significant differences between species tested with a one-way ANOVA followed by a Tukey HSD test.

Despite the spread, a significant trend of deeper scour holes with increasing stem diameter was observed over all three species characterized by a single stem (Regression analysis: $F_{3,114}$ = 31.08, $p < 0.05$, R^2 = 0.45, non scour-related erosion features were excluded from the analysis)

(Fig. 7). Due to the multiple stems of *P. maritima*, which act more as a tussock, this species was excluded from the analysis. *S. anglica* had the smallest stem diameters. Therefore, scour depth was generally lower compared to *B. maritimus* and *S. tabermaemonatni.*

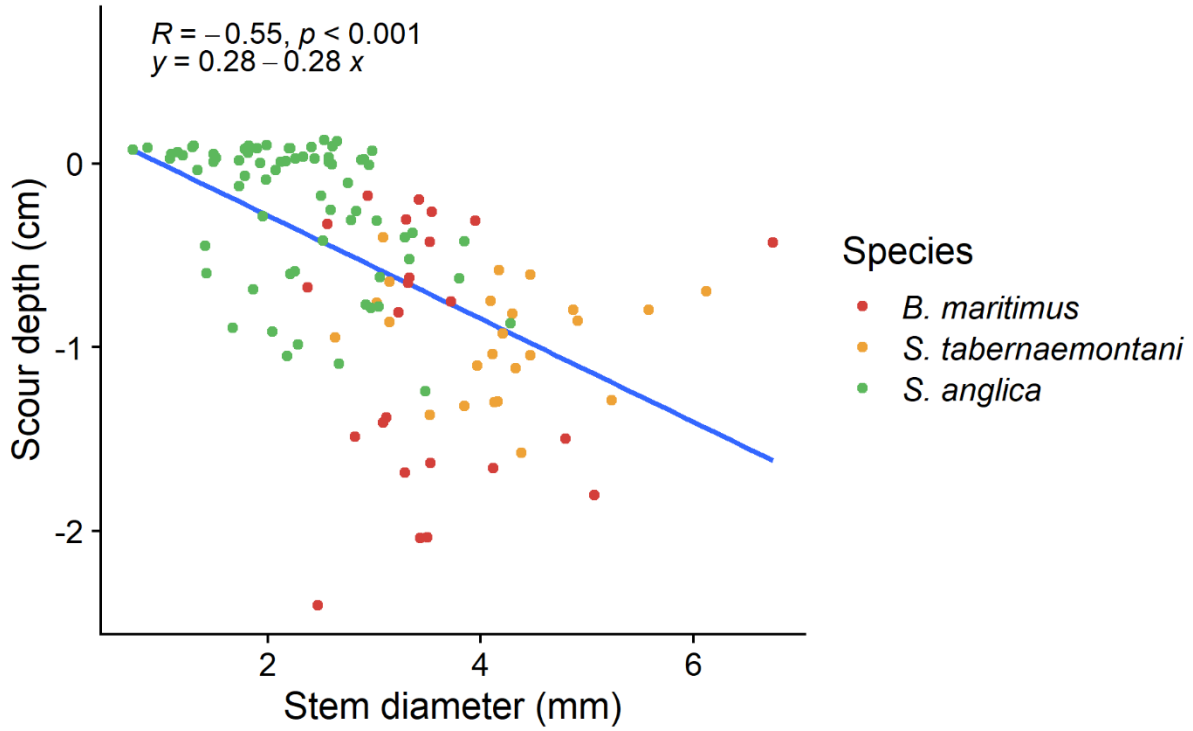

Figure 7: Scour depth (m) plotted against basal stem diameter (mm) across the three single-stem species (*B. maritimus*, *S. tabernaemontani* and *S. anglica*) showed a negative correlation indicated by the Pearson correlation coefficient (*R*).

Discussion

The results of this large wave-flume experiment show that the survival rate of seedlings in response to storm waves is plant trait dependent. More specifically, seedling survival decreases when the seedling has plant traits that increase the potential drag force and scouring around the stem. This knowledge has multiple implications for marsh (re-)establishment and should be

taken into consideration when modeling and planning tidal marsh restoration and creation projects.

Plant-trait dependent loss of seedling shoots

Both *B. maritimus* and *S. tabernaemontani* showed a similarly high loss of shoots, while this was negligible for *S. anglica* and *P. maritima* (Fig. 2). Dislodgement is considered the main cause of death for young seedlings during germination and the initial establishment phase, even under calm wave conditions (Balke et al. 2013; Zhu et al. 2014; Cao et al. 2018). However, in this study we did not observe complete dislodgment of seedlings, including their roots, under storm wave conditions. All observed losses of *B. maritimus* and *S. tabernaemontani* shoots happened through basal stem breakage, predominantly at the connection between the stem and the roots. It is known from previous studies that long shoots increase the drag forces pulling on the stems which makes them more vulnarable to breaking (Albayrak et al. 2014). Hence our results confirm that the higher loss rate by stem breakage for *B. maritimus* and *S. tabernaemontani* seedlings (Fig. 2), is related to their significantly higher shoot lengths as compared to the two other species in our experiments (Fig. 5). Stem breakage of adult shoots of these two species mainly occurs several centimeters above the sediment surface at the end of the growing season when the shoots are deteriorating as part of the seasonal growth cycle (Vuik et al. 2018; Schoutens et al. 2019; Zhu et al. 2019). Our experiments show that seedling stems typically first bend and then break at the shoot-root interface. It should be noted that the question of whether shoot breakage leads to permanent loss of the seedlings, cannot be confirmed from our experiments. The ability of a shoot to break close to the root connection may be seen as a strategy to avoid drag forces and scouring, while the remaining root network might prevent the sediment surface from eroding (Spencer et al. 2016; Wang et al. 2017). Hence, damage by stem breakage in the short term could reduce the risk for complete root dislodgement, thus allowing regrowth of shoots from the roots and facilitating seedling survival

over the longer term. Such a survival strategy by stem breaking under storm waves and regrowth from surviving roots was also suggested by Rupprecht et al. (2017) for an adult canopy of the high marsh species *Elymus athericus*. Fast regrowth of shoots is also what we observed from the cut-off outgrown shoots of *B. maritimus* and *S. tabernaemontani* (see supplementary figure 1).

Plant trait dependent bending of shoots

Applying a wide range of different wave runs with different wave conditions allowed us to demonstrate that species-specific responses also depend on the wave conditions (Fig. 2). The calmest wave conditions in this experiment show very small (or no) differences in species response while heavier wave conditions show increaslingly larger species-specific responses. This proves that it are the more extreme wave conditions that are most selective in terms of species response. *B. maritimus* suffered the most among all studied species with bent shoots or shoots lying flat on the sediment surface after an accumulative wave loading of ≥ 132 Js (Fig. 2). Here, we argue that this species-dependent difference in shoot bending may be the result of two mechanisms: scouring around stems and drag forces exerted by the waves on the stems. First, the seedlings of *B. maritimus*, with greatest bending angles (Fig. 2), also had the deepest scour holes (Fig. 3), which resulted in partial uprooting. This suggests that the loss of the anchoring strength of the roots may have contributed to reduced ability of the shoots to keep an upstanding position. Although scour holes around *S. tabernaemontani* were of similar dimensions (Fig. 3), no uprooting was observed indicating that the root system of this species develops at several centimeters below the sediment surface. As *S. tabernaemontani* did not experience uprooting, this may partly explain why it also experienced less bending as compared to *B. maritimus* seedlings. *S. anglica* and *P. maritima* showed least percentages of shoot bending (Fig. 2) and lowest scouring depths (Fig. 3). Overall, this suggests that shoot bending is positively related to the depth of scouring holes across the studied species.

Moreover, our results showed that across the studied species, the scouring depth is deeper around stems with a larger diameter (Fig. 7). Here, it should be noted that although *S. anglica* had thicker stem diameters, the seedlings of *P. maritima* form grass clumps with multiple stems sprouting from the crown which will likely act as one entity causing more turbulence and thus more scour compared to *S. anglica*. Scour is the result of the interaction between hydrodynamics (wave induced currents in this experiment) and a physical obstacle (seedlings in this experiment) that creates turbulent flow. Since hydrodynamic forces were the same for all seedlings, the stem shape was the key variable to explain the observed differences in scouring depth. It has been shown that the dimensions of scour holes are related to the diameter of the obstacle (Bouma et al. 2009a). Additionally and in accordance with literature, thicker stems were found to have a higher flexural stiffness, which limits their tendency to bend over with the flow. Interestingly, studies on scouring around engineered structures, like bridge pillars, showed that when the angle of the obstacle to the incoming flow is wider, i.e. the obstacle is bent over in the direction of the flow, the turbulence generated around the object changes and creates less deep scouring compared to objects of the same dimensions that stand perpendicular against the flow (Kitsikoudis et al. 2017). Applying this to plant shoots, stiffer stems, that have more tendency to stand perpendicular against the flow, will generate deeper scour holes compared to more flexible stems that bend over to reduce the angle with respect to the flow direction (Bouma et al. 2009a; Yagci et al. 2016).

Secondly, to explain why *B. maritimus* suffers much more from structural bending of the stem compared to *S. tabernaemontani*, we also consider the expected drag forces acting on the seedlings. Both stem diameters and stem lengths are similar for both species, however, an important difference is the aboveground biomass, which is almost double for *B. maritimus* as compared to the biomass of *S. tabernaemontani* (Fig. 5). The absence of leaves in *S. tabernaemontani* lowers their aboveground biomass which reduces the frontal area and hence,

is expected to reduce the experienced drag (Paul et al. 2016; Silinski et al. 2016). *S. anglica* and *P. maritima* do have leaves, but these were small (Fig 5 and 6) and thus contribute little to the expected drag forces (Paul et al. 2016; Vuik et al. 2018). Apart from aboveground biomass, a higher shoot stiffness is also expected to result in increased drag force and to induce more wave-induced damage on the stem (Rupprecht 2017). Our results also indicate that flexural stem stiffness was highest for the *B. maritimus* and *S. tabernaemontani* (Fig. 6a), which were the species that showed the highest percentages of stem bending (Fig. 2). Overall, our result confirm that plant traits responsible for an increase of drag forces, also increase the damage experienced by the seedling.

The role of a root network

All four species in this experiment are able to grow clonally by producing an extended root network of rhizomes or, in the case of *P. maritima*, aboveground stolons (Charpentier and Stuefer 1999; Sosnová et al. 2010; Silinski et al. 2016). During the experiment, the seedlings were between 10 and 14 weeks old which for *B. maritimus* and *S. tabernaeomontani* had resulted in clonal outgrowth and well developed roots (Fig. 5d and 5e). Although outgrown shoots were cut off prior to the wave runs, the belowground network of rhizomes was able to maintain an anchoring capacity that was strong enough to avoid complete uprooting during the experiment. Hence, despite their age which results in a more developed shoot that increases the drag forces, a more developed belowground biomass (Fig. 5e) seems to compensate this increased stress (Balke et al. 2013; Cao et al. 2020). It is known from other ecosystems that anchoring capacity is positively correlated with root properties such as rooting depth, structural complexity and root biomass (Peralta et al. 2006; Schwarz et al. 2010; Edmaier et al. 2014), but research on root networks in tidal marsh vegetation remains sparse (Friess et al. 2012). Apart from the root properties of the seedlings, the cohesiveness of the sediment bed plays a role in the anchoring capacity and resistance against dislodgement of the seedlings (Edmaier

et al. 2014; Schwarz et al. 2015; Lo et al. 2017). Highly cohesive sediments have a higher shear strength which prevents erosion (e.g. scouring) and potential uprooting, even under storm wave conditions (Möller et al. 2014; Spencer et al. 2016). The sediment used in this experiment was fairly cohesive (32% < 63 μm), implying that erosion and uprooting might have been more prominent in less cohesive, more sandy sediment. Fast developing belowground root networks are likely to be an important survival strategy of developing seedlings, which may facilitate marsh establishment. Moreover, root development is regulated by multiple environmental variables such as oxygen limitation (Bouma et al. 2001), bioturbation and salt stress, which are conditions that were not varied in this study. Therefore, detailed studies of the root development in the first growing season with a focus on rooting depth and outgrowth by rhizomes can provide crucial insights into spatial and temporal patterns of colonisation and survival of marsh plant seedlings (Balke et al. 2014; Cao et al. 2018, 2020).

Simulated storm-wave and local environmental conditions

The hydrodynamics created in this experiment were simulating storm waves that matched or exceeded most severe wave conditions measured in the field in marsh pioneer zones (Table 1). Important to note is that storm wave exposure under field conditions has a duration of multiple hours which is longer than the short term exposure in this experiment. Moreover, water depths in this study (1.5 m) were rather deep. Although such water depths may indeed typically occur during storm surges at the moment of peak water level (Table 2), tidal water level variations in marsh pioneer zones may also lead to storm wave conditions coinciding with much shallower water depths. Therefore, it should be noted that even higher shear stress can be expected under storm conditions coinciding with more shallow water and breaking wave conditions (Fagherazzi and Wiberg 2009; Leonardi et al. 2015; Pascolo et al. 2018).

Interestingly, the two species that were most damaged (i.e. *S. tabernaemontani* and *B. maritimus)*, grow in the brackish water zone of estuaries. Along estuarine salt gradients, the brackish water zone is more upstream, where open water surfaces are typically smaller, and thus wind fetch length and wave loading during storms are expected to be smaller. The two species that were least affected in our experiments (i.e. *P. maritima* and *S. anglica*), grow in the salt water zone, in what are often more exposed areas closer to the mouth of estuaries where storms energies are higher (Van der Wal et al. 2008; Callaghan et al. 2010; Yang et al. 2012). This suggests that the natural hydrodynamic growth conditions of the species may have played a role in the selection of species traits that allow salt marsh plants to cope better with storm waves as compared to brackish marsh species, althoug many other factors such as tolerance to salt stress will play a role, and more research is needed to further investigate this hypothesis. For example, studies on adult plants have already shown different responses to hydrodynamic forces in relation to their species-specific plant traits (e.g. Bouma et al. 2010; Silinski et al. 2016a; Rupprecht et al. 2017; Vuik et al. 2018; Zhu et al. 2019; Schoutens et al. 2020).

Implications for planning of marsh restoration and creation

Our results indicate that, depending on the pioneer marsh species, storm wave events can be a bottleneck for the success of marsh establishment in the first growing season. This has implications for the selection and design of suitable marsh restoration or creation sites, a practice that is frequently adopted to enhance or increase the delivery of valuable ecosystem services such as biodiversity conservation, coastal defense, and carbon sequestration (Barbier et al. 2011). Apart from well-documented site characteristics, such as suitable intertidal elevation and soil conditions (Wolters et al. 2008; Zhao et al. 2020), and proximity to existing marshes for seed dispersal (Morzaria-Luna and Zedler 2007; Zhu et al. 2014), our findings stress that site exposure to risks of storm waves is one of the factors that should be taken into account in marsh restoration or creation projects. The latter is expected to become increasingly

relevant, as in many coastal areas, storm activity is expected to increase over the coming decades due to climate change (Bender et al. 2010; Vitousek et al. 2017; Habel et al. 2020),

From our findings it becomes evident that, when planning and designing sites for marsh restoration and creation projects, it is important to evaluate the risk of damage and disturbance cauased by storm waves beyond an initial window of opportunity for seed dispersal and germination (Bouma et al. 2014). For example, tidal marsh creation in a brackish water environment, where the pioneer species are *B. maritimus* and *S. tabernaemontani*, will be more vulnarable to storm waves in the first growing season. In contrast, the seedlings of pioneer salt water species such as *S. anglica* and *P. maritima* are better able to withstand the storm waves. Moreover we argue that, depending on the location, a low disturbance period for seed germination (i.e. previously identified to be 3 days up to 4 weeks, Hu et al. 2015) might not be sufficient for successful marsh establishment, as marsh seedlings (here grown for 10 – 14 weeks) can still be disrupted by storm waves. Furthermore, the increased storminess due to global climate change might affect the frequency and duration of windows of opportunity for seedling survival and therefore the chance of marsh establishment (Balke et al. 2014). To mitigate the risk for potential disturbance such as through storm wave events, artificial wave damping structures (such as wood branch fences; Dao et al. 2018) can be used to create temporary sheltered conditions, which can facilitate the growth of seedlings into mature plants and improve the success of the restoration. Indeed, over time, the clonal outgrowth and the formation of a root network seems to secure the survival chance of marsh plants. This type of density-dependent feedback through clonal outgrowth and tussock formation is known to contribute importantly to the stability of more mature marshes (Bouma et al. 2009b; Bricker et al. 2018). Hence, temporary fences constructed to create wave sheltered environments so as to facilitate seedling establishment, may be removed after several years once dense vegetation patches have formed.

Finally, knowledge on the impact of extreme wave events on the probability of seedling establishment is often a big uncertainty in predicting marsh establishment, and is consequently not considered in existing marsh evolution models (Mariotti and Fagherazzi 2010; Hu et al. 2015; Poppema et al. 2019). Large scale flume experiments such as reported in this study, can help to better define processes and parameters that need to be included in marsh development models to improve their predictive capability. As pointed out by Hanley et al. (2020), knowledge on the scale of individual plants is crucial to optimize the succes rate of large scale marsh restoration and creation projects that are key to adapt our coastal areas to the predictions of increased storminess.

Acknowledgements

We would like to thank the crew of the Forschungszentrum Küste (FZK) for all the logistic support during the experiment and Lennart van IJzerloo for the support in preparing the sediment boxes and growing the seedlings. We thank Haobing Cao, Rachael Dennis, Jennifer Lustig, Anke van Eggermond, Elizabeth Christie, Helen Brooks and Meline Brendel for their help in the flume and Grazia Doronzo for the analysis of the velocity measurements. This research was financed by the European Union's Horizon 2020 research and innovation program (654110, HYDRALAB+), the Research Foundation Flanders, Belgium (FWO, PhD fellowship for fundamental research K. Schoutens, 1116319N) and the German Research Foundation, Germany (DFG project S. Reents, 401564364). The authors have no conflicts of interest to declare.

References

Albayrak, I., V. Nikora, O. Miler, and M. T. O'Hare. 2014. Flow-plant interactions at leaf,

stem and shoot scales: Drag, turbulence, and biomechanics. Aquat. Sci. **76**: 269–294. doi:10.1007/s00027-013-0335-2

Van Asselen, S., P. H. Verburg, J. E. Vermaat, and J. H. Janse. 2013. Drivers of wetland conversion: A global meta-analysis. PLoS One **8**: 1–13. doi:10.1371/journal.pone.0081292

Balke, T., P. M. J. Herman, and T. J. Bouma. 2014. Critical transitions in disturbance-driven ecosystems : identifying Windows of Opportunity for recovery. J. Ecol. **102**: 700–708. doi:10.1111/1365-2745.12241

Balke, T., E. L. Webb, E. van den Elzen, D. Galli, P. M. J. J. Herman, and T. J. Bouma. 2013. Seedling establishment in a dynamic sedimentary environment: A conceptual framework using mangroves. J. Appl. Ecol. **50**: 740–747. doi:10.1111/1365-2664.12067

Barbier, E. B., S. D. Hacker, C. Kennedy, E. W. Koch, A. C. Stier, and B. R. Silliman. 2011. The value of estuarine and coastal ecosystem services. Ecol. Monogr. **81**: 169–193. doi:10.1890/10-1510.1

Bender, M. A., T. R. Knutson, R. E. Tuleya, J. J. Sirutis, G. A. Vecchi, S. T. Garner, and I. M. Held. 2010. Modeled Impact of Anthropogenic Warming on the Frequency of Intense Atlantic Hurricanes. Science (80-.). **327**: 454–458. doi:10.1126/science.1180568

Bouma, T. J., J. van Belzen, T. Balke, and others. 2014. Identifying knowledge gaps hampering application of intertidal habitats in coastal protection: Opportunities & steps to take. Coast. Eng. **87**: 147–157. doi:10.1016/j.coastaleng.2013.11.014

Bouma, T. J., M. Friedrichs, P. Klaassen, and others. 2009a. Effects of shoot stiffness, shoot size and current velocity on scouring sediment from around seedlings and propagules. Mar. Ecol. Prog. Ser. **388**: 293–297. doi:10.3354/meps08130

Bouma, T. J., M. Friedrichs, B. K. van Wesenbeeck, S. Temmerman, G. Graf, and P. M. J.

Herman. 2009b. Density-dependent linkage of scale-dependent feedbacks: a flume study on the intertidal macrophyte *Spartina anglica*. Oikos **118**: 260–268. doi:10.1111/j.1600-0706.2008.16892.x

Bouma, T. J., B. P. K. Michel, and K. L. Nielsen. 2001. Coping with low nutrient availability and inundation : root growth responses of three halophytic grass species from different elevations along a flooding gradient. 472–481. doi:10.1007/s004420000545

Bouma, T. J., M. B. De Vries, and P. M. J. Herman. 2010. Comparing ecosystem engineering efficiency of two plant species with contrasting growth strategies. Ecol. Soc. Am. **91**: 2696–2704. doi:10.1890/09-0690.1

Bricker, E., A. Calladine, R. Virnstein, and M. Waycott. 2018. Mega clonality in an aquatic plant—a potential survival strategy in a changing environment. Front. Plant Sci. **9**: 1–8. doi:10.3389/fpls.2018.00435

Callaghan, D. P. P., T. J. J. Bouma, P. Klaassen, D. van der Wal, M. J. F. J. F. Stive, and P. M. J. M. J. Herman. 2010. Hydrodynamic forcing on salt-marsh development: Distinguishing the relative importance of waves and tidal flows. Estuar. Coast. Shelf Sci. **89**: 73–88. doi:10.1016/j.ecss.2010.05.013

Cao, H., Z. Zhu, T. Balke, L. Zhang, and T. J. Bouma. 2018. Effects of sediment disturbance regimes on Spartina seedling establishment: Implications for salt marsh creation and restoration. Limnol. Oceanogr. **63**: 647–659. doi:10.1002/lno.10657

Cao, H., Z. Zhu, R. James, and others. 2020. Wave effects on seedling establishment of three pioneer marsh species: survival, morphology and biomechanics. Ann. Bot. **125**: 345–352. doi:10.1093/aob/mcz136

Charpentier, A., and J. F. Stuefer. 1999. Functional specialization of ramets in *Scirpus maritimus* - Splitting the tasks of sexual reproduction, vegetative growth, and resource storage. Plant Ecol. **141**: 129–136. doi:https://doi.org/10.1023/A:1009825905117

Clark, M. P., B. Nijssen, J. D. Lundquist, and others. 2015. Flow and scour constraints on uprooting of pioneer woody seedlings. 2498–2514. doi:10.1002/2015WR017200.A

Dalrymple, R. A., and R. G. Dean. 1991. Water wave mechanics for engineers and scientists (Vol. 2), Prentice-Hall.

Dao, T., M. J. F. Stive, B. Hofland, and T. Mai. 2018. Wave Damping due to Wooden Fences along Mangrove Coasts. J. Coast. Res. **34**: 1317. doi:10.2112/jcoastres-d-18-00015.1

Denny, M. W. 1994. Extreme drag forces and the survival of wind- and water-swept organisms. J. Exp. Bot. **194**: 97–115.

Duggan-Edwards, M. F., J. F. Pagès, S. R. Jenkins, T. J. Bouma, and M. W. Skov. 2020. External conditions drive optimal planting configurations for salt marsh restoration. J. Appl. Ecol. **57**: 619–629. doi:10.1111/1365-2664.13550

Edmaier, K., B. Crouzy, R. Ennos, P. Burlando, and P. Perona. 2014. Influence of root characteristics and soil variables on the uprooting mechanics of Avena sativa and Medicago sativa seedlings. Earth Surf. Process. Landforms **39**: 1354–1364. doi:10.1002/esp.3587

Elsen, R., A. Van Braeckel, J. Vanoverbeke, B. Vandevoorde, and E. Van den Berg. 2019. Habitatmapping Sea Scheldt supralittoral: Partim pioneer club-rush species. Reports of the Research Institute for Nature and Forest 2019 (36). Research Institute for Nature and For- est , Brussels. doi.org/10.21436/inbor.16164273

Fagherazzi, S., and P. L. Wiberg. 2009. Importance of wind conditions, fetch, and water levels on wave-generated shear stresses in shallow intertidal basins. J. Geophys. Res. Earth Surf. **114**: 1–12. doi:10.1029/2008JF001139

Friess, D. a, K. W. Krauss, E. M. Horstman, T. Balke, T. J. Bouma, D. Galli, and E. L. Webb. 2012. Are all intertidal wetlands naturally created equal? Bottlenecks, thresholds and knowledge gaps to mangrove and saltmarsh ecosystems. Biol. Rev. Camb. Philos. Soc.

87: 346–66. doi:10.1111/j.1469-185X.2011.00198.x

Habel, S., C. H. Fletcher, T. R. Anderson, and P. R. Thompson. 2020. Sea-Level Rise Induced Multi-Mechanism Flooding and Contribution to Urban Infrastructure Failure. Sci. Rep. **10**: 1–12. doi:10.1038/s41598-020-60762-4

Hanley, M. E., T. J. Bouma, and H. L. Mossman. 2020. The gathering storm : optimizing management of coastal ecosystems in the face of a climate-driven threat. Ann. Bot. **125**: 197–212. doi:10.1093/aob/mcz204

Hansen, F., T. Kruschke, R. J. Greatbatch, and A. Weisheimer. 2019. Factors Influencing the Seasonal Predictability of Northern Hemisphere Severe Winter Storms. Geophys. Res. Lett. **46**: 365–373. doi:10.1029/2018GL079415

Henry, P. Y., D. Myrhaug, and J. Aberle. 2015. Drag forces on aquatic plants in nonlinear random waves plus current. Estuar. Coast. Shelf Sci. **165**: 10–24. doi:10.1016/j.ecss.2015.08.021

Heuner, M., B. Schröder, U. Schröder, and B. Kleinschmit. 2018. Contrasting elevational responses of regularly flooded marsh plants in navigable estuaries. Ecohydrol. Hydrobiol. **19**: 38–53. doi:10.1016/j.ecohyd.2018.06.002

Hu, Z., J. van Belzen, D. van der Wal, T. Balke, Z. B. Wang, M. Stive, and T. J. Bouma. 2015. Windows of opportunity for salt marsh vegetation establishment on bare tidal flats: The importance of temporal and spatial variability in hydrodynamic forcing. J. Geophys. Res. Biogeosciences **120**. doi:10.1002/2014JG002870.Received

Kitsikoudis, V., V. S. O. Kirca, O. Yagci, and M. F. Celik. 2017. Clear-water scour and flow field alteration around an inclined pile. Coast. Eng. **129**: 59–73. doi:10.1016/j.coastaleng.2017.09.001

Lague, D., N. Brodu, and J. Leroux. 2013. Accurate 3D comparison of complex topography with terrestrial laser scanner: Application to the Rangitikei canyon (N-Z). ISPRS J.

Photogramm. Remote Sens. **82**: 10–26. doi:10.1016/j.isprsjprs.2013.04.009

Leonardi, N., N. K. Ganju, and S. Fagherazzi. 2015. A linear relationship between wave power and erosion determines salt-marsh resilience to violent storms and hurricanes. Proc. Natl. Acad. Sci. **113**: 64–68. doi:10.1073/pnas.1510095112

Lo, V. B., T. J. Bouma, J. van Belzen, C. Van Colen, and L. Airoldi. 2017. Interactive effects of vegetation and sediment properties on erosion of salt marshes in the Northern Adriatic Sea. Mar. Environ. Res. **131**: 32–42. doi:10.1016/j.marenvres.2017.09.006

Lotze, H. K., H. S. Lenihan, B. J. Bourque, and others. 2006. Depletion, Degradation, and Recovery Potential of Estuaries and Coastal Seas. Science (80-.). **312**: 1806–1809. doi:10.1126/science.1128035

Mariotti, G., and S. Fagherazzi. 2010. A numerical model for the coupled long-term evolution of salt marshes and tidal flats. J. Geophys. Res. **115**: F01004. doi:10.1029/2009JF001326

Masselink, G., T. Scott, T. Poate, P. Russell, M. Davidson, and D. Conley. 2016. The extreme 2013/2014 winter storms: Hydrodynamic forcing and coastal response along the southwest coast of England. Earth Surf. Process. Landforms **41**: 378–391. doi:10.1002/esp.3836

Möller, I., M. Kudella, F. Rupprecht, and others. 2014. Wave attenuation over coastal salt marshes under storm surge conditions. Nat. Geosci. **7**: 727–731. doi:10.1038/ngeo2251

Möller, I., T. Spencer, J. R. French, D. J. Leggett, and M. Dixond. 1999. Wave Transformation Over Salt Marshes: A Field and Numerical Modelling Study from North Norfolk, England. Estuar. Coast. Shelf Sci. **49**: 411–426. doi:10.1006/ecss.1999.0509

Morzaria-Luna, H. N., and J. B. Zedler. 2007. Does seed availability limit plant establishment during salt marsh restoration? Estuaries and Coasts **30**: 12–25. doi:10.1007/BF02782963

Narayan, S., M. W. Beck, B. G. Reguero, and others. 2016. The Effectiveness, Costs and

Coastal Protection Benefits of Natural and Nature-Based Defences. PLoS One **11**: e0154735. doi:10.1371/journal.pone.0154735

van der Nat, A., P. Vellinga, R. Leemans, and E. van Slobbe. 2016. Ranking coastal flood protection designs from engineered to nature-based. Ecol. Eng. **87**: 80–90. doi:10.1016/j.ecoleng.2015.11.007

Nicholls, R. J., and A. Cazenave. 2010. Sea-Level Rise and Its Impact on Coastal Zones. Science (80-.). **328**: 1517–1520. doi:10.1126/science.1185782

Niklas, K. J. 1992. Plant biomechanics: An engineering approach to plant form and function, The University of Chicago Press.

Oppenheimer, M., B. Glavovic, J. Hinkel, and others. 2019. Sea Level Rise and Implications for Low Lying Islands, Coasts and Communities. IPCC Spec. Rep. Ocean Cryosph. a Chang. Clim. **355**: 126–129. doi:10.1126/science.aam6284

Pascolo, S., M. Petti, and S. Bosa. 2018. On the wave bottom shear stress in shallow depths: The role of wave period and bed roughness. Water (Switzerland) **10**. 1348–1367. doi:10.3390/w10101348

Paul, M., F. Rupprecht, I. Möller, and others. 2016. Plant stiffness and biomass as drivers for drag forces under extreme wave loading: A flume study on mimics. Coast. Eng. **117**: 70–78. doi:10.1016/j.coastaleng.2016.07.004

Peralta, G., F. G. Brun, J. L. Pérez-Lloréns, and T. J. Bouma. 2006. Direct effects of current velocity on the growth, morphometry and architecture of seagrasses: A case study on *Zostera noltii*. Mar. Ecol. Prog. Ser. **327**: 135–142. doi:10.3354/meps327135

Poppema, D. W., P. W. J. M. Willemsena, M. B. de Vries, Z. Zhu, B. W. Borsje, and S. J. M. H. Hulscher. 2019. Experiment - supported modelling of salt marsh establishment. Ocean Coast. Manag. **168**: 238–250.

R Core Team. 2019. R: A language and environment for statis- tical computing. Vienna,

Austria: R Foundation for Statisti- cal Computing. https://www.R-project.org/

Rupprecht, F., I. Möller, B. Evans, T. Spencer, and K. Jensen. 2015. Biophysical properties of salt marsh canopies — Quantifying plant stem flexibility and above ground biomass. Coast. Eng. **100**: 48–57. doi:10.1016/j.coastaleng.2015.03.009

Rupprecht, F., I. Möller, M. Paul, and others. 2017. Vegetation-wave interactions in salt marshes under storm surge conditions. Ecol. Eng. **100**: 301–315. doi:10.1016/j.ecoleng.2016.12.030

Schoutens, K., M. Heuner, E. Fuchs, V. Minden, T. Schulte-Ostermann, J. P. Belliard, T. J. Bouma, and S. Temmerman. 2020. Nature-based shoreline protection by tidal marsh plants depends on trade-offs between avoidance and attenuation of hydrodynamic forces. Estuar. Coast. Shelf Sci. **236**: 11. doi:10.1016/j.ecss.2020.106645

Schoutens, K., M. Heuner, V. Minden, T. Schulte Ostermann, A. Silinski, J.-P. Belliard, and S. Temmerman. 2019. How effective are tidal marshes as nature-based shoreline protection throughout seasons? Limnol. Oceanogr. **64**: 1750–1762. doi:10.1002/lno.11149

Schwarz, C., T. J. Bouma, L. Q. Zhang, S. Temmerman, T. Ysebaert, and P. M. J. Herman. 2015. Interactions between plant traits and sediment characteristics influencing species establishment and scale-dependent feedbacks in salt marsh ecosystems. Geomorphology **250**: 298–307. doi:10.1016/j.geomorph.2015.09.013

Schwarz, M., D. Cohen, and D. Or. 2010. Root-soil mechanical interactions during pullout and failure of root bundles. J. Geophys. Res. Earth Surf. **115**: 1–19. doi:10.1029/2009JF001603

Silinski, A., E. Fransen, J. van Belzen, and others. 2016. Quantifying critical conditions for seaward expansion of tidal marshes: A transplantation experiment. Estuar. Coast. Shelf Sci. **169**: 227–237. doi:10.1016/j.ecss.2015.12.012

Silinski, A., M. Heuner, J. Schoelynck, and others. 2015. Effects of wind waves versus ship waves on tidal marsh plants: A flume study on different life stages of *Scirpus maritimus*. PLoS One **10**: e0118687. doi:10.1371/journal.pone.0118687

Silinski, A., K. Schoutens, S. Puijalon, J. Schoelynck, D. Luyckx, P. Troch, P. Meire, and S. Temmerman. 2018. Coping with waves: Plasticity in tidal marsh plants as self-adapting coastal ecosystem engineers. Limnol. Oceanogr. **63**: 799–815. doi:10.1002/lno.10671

Sosnová, M., R. van Diggelen, and J. Klimešová. 2010. Distribution of clonal growth forms in wetlands. Aquat. Bot. **92**: 33–39. doi:10.1016/j.aquabot.2009.09.005

Spencer, T., S. M. Brooks, B. R. Evans, J. A. Tempest, and I. Möller. 2015. Southern North Sea storm surge event of 5 December 2013 : Water levels , waves and coastal impacts. Earth Sci. Rev. **146**: 120–145. doi:10.1016/j.earscirev.2015.04.002

Spencer, T., I. Möller, F. Rupprecht, and others. 2016. Salt marsh surface survives true-to-scale simulated storm surges. Earth Surf. Process. Landforms **41**: 543–552. doi:10.1002/esp.3867

Szmeja, J., and A. Galka. 2008. Phenotypic responses to water flow and wave exposure in aquatic plants. Acta Soc. Bot. Pol. **77**: 59–65. doi:https://doi.org/10.5586/asbp.2008.009

Usherwood, J. R., a R. Ennos, and D. J. Ball. 1997. Mechanical and anatomical adaptations in terrestrial and aquatic buttercups to their respective environments. J. Exp. Bot. 48: 1469–1475. doi:10.1093/jxb/48.7.1469

Vitousek, S., P. L. Barnard, C. H. Fletcher, N. Frazer, L. Erikson, and C. D. Storlazzi. 2017. Doubling of coastal flooding frequency within decades due to sea-level rise. Sci. Rep. **7**: 1–9. doi:10.1038/s41598-017-01362-7

Vogel, S. 1996. Life in moving fluids: the physical biology of flow, 2nd ed. Princeton University Press.

Vuik, V., S. N. Jonkman, B. W. Borsje, and T. Suzuki. 2016. Nature-based flood protection:

The efficiency of vegetated foreshores for reducing wave loads on coastal dikes. Coast. Eng. **116**: 42–56. doi:10.1016/j.coastaleng.2016.06.001

Vuik, V., H. Y. Suh Heo, Z. Zhu, B. W. Borsje, and S. N. Jonkman. 2018. Stem breakage of salt marsh vegetation under wave forcing: A field and model study. Estuar. Coast. Shelf Sci. **200**: 41–58. doi:10.1016/j.ecss.2017.09.028

Van der Wal, D., A. Wielemaker-Van den Dool, and P. M. J. Herman. 2008. Spatial patterns, rates and mechanisms of saltmarsh cycles (Westerschelde, The Netherlands). Estuar. Coast. Shelf Sci. **76**: 357–368. doi:10.1016/j.ecss.2007.07.017

Wang, H., D. van der Wal, X. Li, and others. 2017. Zooming in and out: Scale dependence of extrinsic and intrinsic factors affecting salt marsh erosion. J. Geophys. Res. Earth Surf. **122**: 1455–1470. doi:10.1002/2016JF004193

Wolters, M., A. Garbutt, R. M. Bekker, J. P. Bakker, and P. D. Carey. 2008. Restoration of salt-marsh vegetation in relation to site suitability, species pool and dispersal traits. J. Appl. Ecol. **45**: 904–912. doi:10.1111/j.1365-2664.2008.01453.x

Xie, T., B. Cui, S. Li, and J. Bai. 2019. Topography regulates edaphic suitability for seedling establishment associated with tidal elevation in coastal salt marshes. Geoderma **337**: 1258–1266. doi:10.1016/j.geoderma.2018.07.053

Yagci, O., M. F. Celik, V. Kitsikoudis, V. S. Ozgur Kirca, C. Hodoglu, M. Valyrakis, Z. Duran, and S. Kaya. 2016. Scour patterns around isolated vegetation elements. Adv. Water Resour. **97**: 251–265. doi:10.1016/j.advwatres.2016.10.002

Yang, S. L., B. W. Shi, T. J. Bouma, T. Ysebaert, and X. X. Luo. 2012. Wave attenuation at a salt marsh margin : A case study of an exposed coast on the Yangtze Estuary. Estuaries and Coasts **35**: 169–182. doi:10.1007/s12237-011-9424-4

Ysebaert, T., S. Yang, L. Zhang, Q. He, T. J. Bouma, and P. M. J. Herman. 2011. Wave attenuation by two contrasting ecosystem engineering salt marsh macrophytes in the

intertidal pioneer zone. Wetlands **31**: 1043–1054. doi:10.1007/s13157-011-0240-1

Zhao, Z., L. Yuan, W. Li, B. Tian, and L. Zhang. 2020. Re-invasion of Spartina alterniflora in restored saltmarshes: Seed arrival, retention, germination, and establishment. J. Environ. Manage. **266**: 110631. doi:10.1016/j.jenvman.2020.110631

Zhu, Z., T. J. Bouma, T. Ysebaert, L. Zhang, and P. M. J. Herman. 2014. Seed arrival and persistence at the tidal mudflat: Identifying key processes for pioneer seedling establishment in salt marshes. Mar. Ecol. Prog. Ser. **513**: 97–109. doi:10.3354/meps10920

Zhu, Z., V. Vuik, P. J. Visser, and others. 2020. Historic storms and the hidden value of coastal wetlands for nature-based flood defence. Nat. Sustain. doi:10.1038/s41893-020-0556-z

Zhu, Z., Z. Yang, and T. J. Bouma. 2019. Biomechanical properties of marsh vegetation in space and time: effects of salinity, inundation and seasonality. Ann. Bot. doi:10.1046/j.1365-2087.1998.00089.x

Zuur, A. F., E. N. Ieno, N. J. Walker, A. A. Saveliev, and G. M. Smith. 2009. Mixed effects models and extensions in ecology with R, Springer, New York, USA.

Supplementary information: Survival of the thickest? – Impacts of extreme wave-forcing on marsh seedlings are mediated by species morphology

1. Outgrowth and uprooting

Supplementary figure 1: Pictures of the *B. maritimus* seedlings illustrate the partial uprooting of shoots and the point of breakage at the connection between the roots and the stem. Rhizomes ensure the anchoring of the uprooted seedling. In between the seedlings under investigation, other seedlings were growing as a result of clonal outgrowth. These were clipped each day to exclude them from the experiments.

2. Representative current load on plants

Following Madsen (1994), who defined "a representative periodic wave by its near-bottom orbital velocity amplitude u_{br} …" for irregular waves in spectral domain, a similar approach is used here, however, in time domain. Furthermore, the kinetic energy is used to obtain a measure for the cumulative load due to orbital velocity at the investigation zones.

The velocity was measured by ADV-sensors, installed 30 cm in front of the seaward edge of each pallet row, the measurement volume of the sensors was 5 cm above the concrete bottom.

The time series of the horizontal component of orbital velocity were analyzed with zero-down-crossing, thus providing minimum and maximum values for all individual velocity oscillations of the generated irregular waves. Very small oscillations around zero were ignored by applying a threshold band with the size of 0.7 % of ($u_{max} - u_{min}$) of the complete time series. In case a pronounced spike was detected in the recorded signal due to a disturbance in the measurement, this event was manually removed from the list of velocity oscillations. From the corrected list the average of positive (u_c, crest) and negative (u_t, trough) maximum velocities were calculated and an average velocity amplitude u_{br} was derived:

$$u_{br} = \frac{1}{2}\left(\frac{1}{n}\sum u_c + \frac{1}{n}\left|\sum u_t\right|\right)$$

With n Number of detected waves

u_c Maximal positive velocity of an individual wave [m/s]

u_t Maximal negative velocity of an individual wave [m/s]

This value is very close to the value calculated in frequency domain by Madsen (1994), here reduced to uni-directional flow:

$$u_{br} = \sqrt{2 \int S_{ub}(\omega) d\omega}$$

With ω radian frequency $= 2\pi f$, f is the frequency

S_{ub} velocity spectrum [(m/s)²s]

In order to find a representative time T_r for the period of the orbital velocity, the following approach is used. A sinusoidal wave with the amplitude u_{br} and the period T_m is considered. T_m is the average period of all velocity oscillations in the selected time interval. As positive and negative velocities both have to be considered as loading cases for the plants and because the sine function is point symmetric, 2 times the integral from 0 to $t=T_m/2$ is considered as velocity load for the representative velocity oscillation:

$$2 \int_0^t u_{br} \sin\left(\frac{2\pi}{T} t\right) dt = -2u_{br} \frac{T_m}{2\pi} \cos\frac{2\pi}{T} t = 2u_{br} \frac{T_m}{\pi} \left(\text{for } t = \frac{T_m}{2}\right)$$

The representative period T_r is considered as the duration of a rectangular load with the same area as the integral given above:

$$u_{br} T_r = 2u_{br} \frac{T_m}{\pi}$$

$$T_r = \frac{2T_m}{\pi} = 0.637 \cdot T_m$$

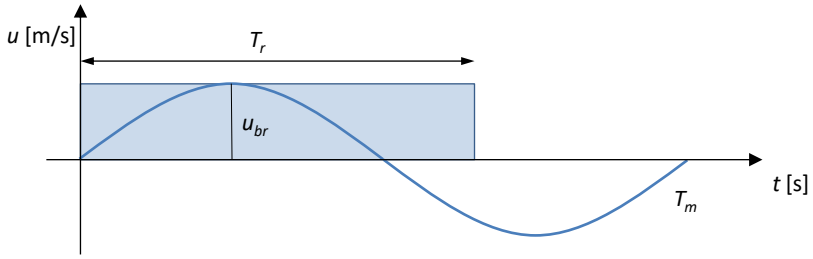

In order to derive a meaningful parameter which includes the duration of velocity load, the kinetic energy $\boldsymbol{E}_{kin,r}$ of the representative orbital velocity is considered:

$$E_{kin,r} = \frac{m \cdot u_{br}^2}{2}$$

With m unit mass of 1 kg

In physics energy times the duration is known as action *S* with the unit Joule-second [Js]. As duration *t*, where the velocity is affecting the plants, the number of detected oscillations *n* multiplied with the representative period T_r is determined. For a wave sequence with *n* velocity oscillations the action *S* can then be calculated as

$$S = E_{kin,r} \cdot t = \frac{1 \cdot u_{br}^2}{2} \cdot nT_r$$

It should be noted that the action *S* alone is not sufficient as measure for the wave load, because the same *S* can be obtained by a long duration with small energy and a short duration with high energy, while the latter will have more impact on plant behavior than the first. In the context of this study, S can be used for comparison, as all wave runs were composed of 1000 waves.

References:

Madsen, O.S. (1994) Spectral Wave-Current Bottom Boundary Layer Flows, 24th International Conference on Coastal Engineering, Kobe, Japan

3. Stress-strain curve

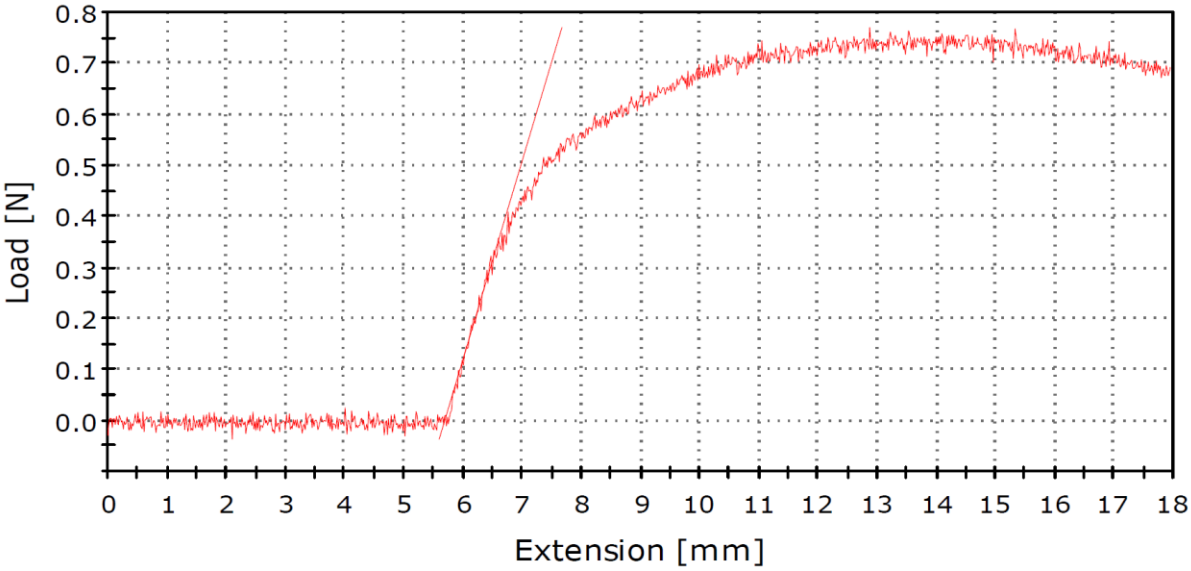

Supplementary figure 2: Stress-strain curve (red curve) generated by the Instron Bleuhill 3.0 software from a three-point bending test on the basal stem part of a *S. tabernaemontani* seedling. The curve describes the relation between vertical deflection of the stem (Extension; on the X-axis) and the bending force of the stem (Load; on the Y-axis) which enables the calculation of the slope from the elastic deformation zone on the curve (F/D). This calculation was done automatically by the soft